JACC: BASIC TO TRANSLATIONAL SCIENCE VOL. 8, NO. 7, 2023


ORIGINAL RESEARCH - PRECLINICAL

# Bag3 Regulates Mitochondrial Function and the Inflammasome Through Canonical and Noncanonical Pathways in the Heart

JuFang Wang, MD,[a,b] Dhadendra Tomar, PhD,[c] Thomas G. Martin, PhD,[d] Shubham Dubey, PhD,[a] Praveen K. Dubey, PhD,[a] Jianliang Song, MD, PhD,[a,b] Gavin Landesberg, BS,[a,b] Michael G. McCormick, MS,[a] Valerie D. Myers, PhD,[e] Salim Merali, PhD,[f] Carmen Merali, BS,[f] Bonnie Lemster, MPH,[g] Charles F. McTiernan, PhD,[g] Kamel Khalili, PhD,[b] Muniswamy Madesh, PhD,[h] Joseph Y. Cheung, MD, PhD,[i] Jonathan A. Kirk, PhD,[d] Arthur M. Feldman, MD, PhD[a,b]

## VISUAL ABSTRACT

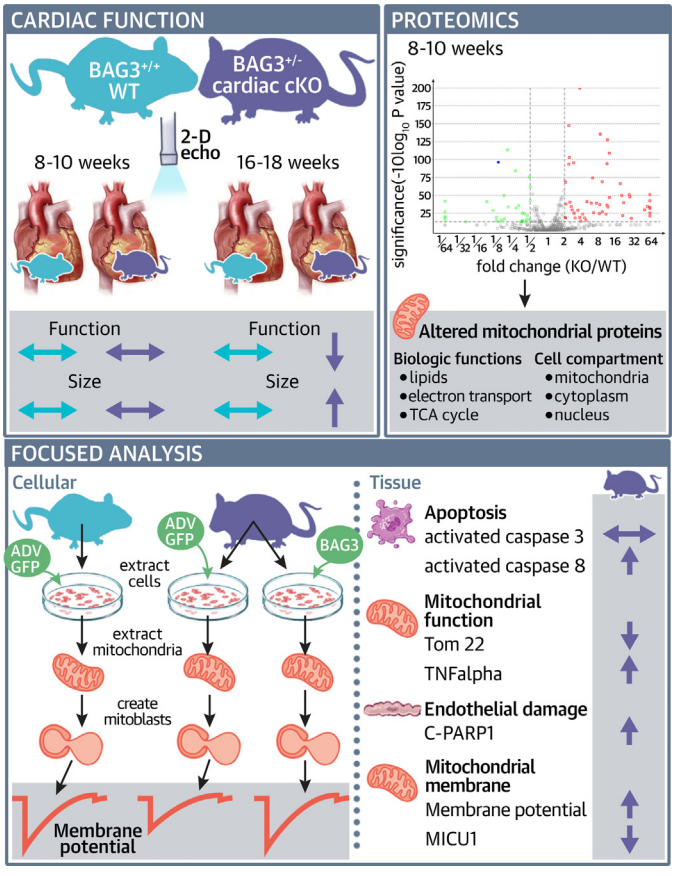


Wang J, et al. J Am Coll Cardiol Basic Trans Science. 2023;8(7):820-839.

## HIGHLIGHTS

- Mice with heterozygous knockout of Bag3 are phenotypically normal by echocardiography at 8 to 10 weeks of age but show marked changes in left ventricular function by 18 weeks of age.
- Evaluation of the proteome of 8- to 10-week-old Bag3$^{+/-}$ mice revealed abnormalities in proteins associated with metabolism and programmed cell death or apoptosis despite a normal phenotype.
- Bag3 regulates cellular apoptosis both through canonical as well as noncanonical pathways.
- Bag3 interacts directly with the inhibitor of apoptosis protein 1/2 (cIAP1/2 or cIAP), the mitochondrial import receptor subunit TOM22, and the $Ca^{2+}$ uniporter in regulating cellular apoptosis and inflammation, mitochondrial metabolism, and the generation of the mitochondrial membrane potential, respectively.
- Decreased levels of Bag3 cause a shift from a balance between the intrinsic and extrinsic pathways of caspase activation to signaling that favors activation of caspase-8.
- Bag3 is indispensable to the health of a cell because it serves as a molecular glue that maintains key proteins in specific microdomains that are critical for normal physiology in high-functioning cells.

ISSN 2452-302X https://doi.org/10.1016/j.jacbts.2022.12.013

## SUMMARY

B-cell lymphoma 2-associated athanogene-3 (Bag3) is expressed in all animal species, with Bag3 levels being most prominent in the heart, the skeletal muscle, the central nervous system, and in many cancers. Preclinical studies of Bag3 biology have focused on animals that have developed compromised cardiac function; however, the present studies were performed to identify the pathways perturbed in the heart even before the occurrence of clinical signs of dilatation and failure of the heart. These studies show that hearts carrying variants that knockout one allele of *BAG3* have significant alterations in multiple cellular pathways including apoptosis, autophagy, mitochondrial homeostasis, and the inflammasome. (J Am Coll Cardiol Basic Trans Science 2023;8:820–839)


Bcl2-associated athanogene-3 (Bag3) is a multifunctional protein that was first cloned more than 2 decades ago. Bag3 expressed ubiquitously, but it is most prominent in the heart, the skeletal muscles, the central nervous system, and in many cancers.[1-4] Multiple genome-wide association studies and whole-exome or whole-genome sequencing of DNA from patients with both hereditary and sporadic dilated cardiomyopathy (DCM) have shown that loss of a single allele of Bag3 is an important cause of DCM.[5-8] This has been confirmed in murine models. Homozygous deletion of Bag3 is lethal in mice, whereas the loss of a single allele leads to the development of cardiac dysfunction and a shortened lifespan.[5,9] Informative point mutations have also been associated with diminished left ventricular (LV) function in mesenchymal stem cell-derived cardiac myocytes, in mice, and in humans.[10-14] Studies have also shown that patients with heart failure with reduced ejection fraction (HFrEF) who harbor no known Bag3 mutants have a reduction in Bag3 in the ventricular myocardium at the time of heart transplantation that is comparable to that observed in patients with Bag3 truncations.[13,14]

A characteristic feature of Bag3 is that it has numerous protein-protein binding domains that allow it to influence a diverse array of molecular and cellular activities.[15] For example, Bag3 augments autophagy by serving as a chaperone to heat shock protein 70 (HSP70/HSC70) and inhibits apoptosis by binding with the anti-apoptosis protein Bcl-2.[15-18] A PXXP domain serves as a molecular anchor for the proximal end of the motor-dynein transport system that takes misfolded proteins to the perinuclear aggresomes. Two isoleucine-proline-valine motifs bind the small heat shock proteins HSPB6 and HSPB8 and support macro-autophagy.[3] Bag3 modulates excitation-contraction coupling by linking the beta-adrenergic receptor and the L-type $Ca^{2+}$ channel, and maintains the integrity of the sarcomere by coupling the actin filaments to the Z-disc.[17,18]

Recent studies in animal models have begun to link specific heterozygous genetic variants in Bag3 with unique cellular or molecular phenotypes. For example, the E455K loss of function mutation disrupts the interaction between Bag3 and

## ABBREVIATIONS AND ACRONYMS

**$\Delta\Psi_m$** = mitochondrial membrane potential

**Bag3** = Bcl2-associated athanogene-3

***BAG3*** = the gene that encodes Bag3

**Bcl2** = B-cell lymphoma 2

**cIAP** = cellular inhibitor of apoptosis (1 and 2 equivalent)

**DCM** = dilated cardiomyopathy

**HFrEF** = heart failure with reduced ejection fraction

**HSP** = heat shock protein

**HuR** = human receptor R

**IMM** = internal mitochondrial membrane

**MICU1** = mitochondrial calcium uptake protein 1

**MICU2** = mitochondrial calcium uptake protein 2

**NMVC** = neonatal mouse ventricular myocyte

**OMM** = outer mitochondrial membrane

**SMAC** = second mitochondria-derived activator of caspase (encoded by the ***DIABLO*** gene)

**TNF** = tumor necrosis factor

**TNFR** = tumor necrosis factor receptor

**TOMM 22** = translocase of outer mitochondrial membrane

**VDAC** = voltage-dependent anion channel

From the [a]Department of Medicine, Division of Cardiology, Lewis Katz School of Medicine at Temple University, Philadelphia, Pennsylvania, USA; [b]Center for Neurovirology and Gene Editing, Lewis Katz School of Medicine at Temple University, Philadelphia, Pennsylvania, USA; [c]Department of Internal Medicine, Wake Forest University School of Medicine, Winston-Salem, North Carolina, USA; [d]Department of Cell and Molecular Physiology, Loyola University Strich School of Medicine, Maywood, Illinois, USA; [e]Renovacor, Inc, Greenwich, Connecticut, USA; [f]Temple University School of Pharmacy, Philadelphia, Pennsylvania, USA; [g]Department of Medicine, Division of Cardiology, University of Pittsburgh School of Medicine, Pittsburgh, Pennsylvania, USA; [h]Department of Medicine, Center for Precision Medicine, University of Texas Health Science Center at San Antonio, San Antonio, Texas, USA; and the [i]Division of Renal Medicine, Brigham and Women's Hospital, Harvard Medical School, Boston, Massachusetts, USA.

Luisa Mestroni, MD, served as Guest Associate Editor for this paper. Michael Bristow, MD, PhD, served as Guest Editor-in-Chief for this paper.

The authors attest they are in compliance with human studies committees and animal welfare regulations of the authors' institutions and Food and Drug Administration guidelines, including patient consent where appropriate. For more information, visit the Author Center.

Manuscript received July 7, 2022; revised manuscript received December 14, 2022, accepted December 29, 2022.

HSP70 resulting in instability of the heat shock proteins and a loss in protein homeostasis.[11] The rare P209L variant is a dominant gain of function mutation that causes aggregation of itself with HSP70 clients which results in stalling of the HSP70 autophagic network leading to a restrictive cardiomyopathy.[19] By contrast, a P209S variant has been reported in association with a late onset axonal Charcot-Marie-Tooth neuropathy.[20,21]

Although studies have focused on the role of Bag3 in experimental models,[21-24] little is known about the effects of Bag3 on the biology of the heart before the development of the clinical signs and symptoms of HFrEF as both we and others have focused on understanding the biology of Bag3 after symptoms have occurred. This question is of more than academic interest because patients with genetic variants in Bag3 including both truncations and deletions do not come to the attention of medical personnel until reaching an average age of 38 years. Therefore, in the present study, we sought to gain a better understanding of the role of Bag3 before the onset of diminished LV function by taking advantage of young transgenic mice between 8 and 10 weeks of age in whom one allele of Bag3 was ablated.[12] We report for the first time that the proteome of young $Bag3^{+/-}$ mice is heavily weighted towards proteins associated with mitochondrial metabolism and the extrinsic pathway of apoptosis when compared with that of nontransgenic (wild-type [WT]) littermate controls.

Understanding the full capabilities of this multifunctional protein is of importance as numerous investigative groups and biotechnology companies are now developing both small molecule and gene therapy approaches to modify Bag3 function and levels for the treatment of a variety of human diseases including DCM, neurodegenerative diseases, and cancer.

## METHODS

The experiments undertaken to evaluate the central hypotheses of this work were often technically and methodologically complex. To meet space constraints, we have provided a full description of each method and lists of the requisite materials including sources for reagents in the expanded Material and Methods section of the Supplemental Appendix.

**ANIMALS, ANIMAL MODELS, SURGICAL PROCEDURES, AND HUMAN TISSUE.** Mice in which a single allele or 2 alleles of Bag3 were deleted were generated by crossing mice carrying a floxed Bag3 ($Bag3^{flox/flox}$) with Cre mice carrying α-myosin heavy chain (all on a C57Bl/6 background) as previously described.[12] $Bag3^{flox/flox.}$ mice (Bag3 [HEPD0556_7_B06]) were obtained from MRC Harwell, a member of the International Mouse Phenotyping Consortium that generates and distributes transgenic mice on behalf of the European Mouse Mutant Archive. The phenotypes of the $Bag3^{+/-}$ and $Bag3^{-/-}$ mice were described previously.[12] Because of their very short lifespan, $Bag3^{-/-}$ mice were only used for breeding purposes and in several experiments when we sought to have a total knockout of Bag3 because results from the loss of a single allele were not informative.

Samples of failing and nonfailing human hearts were obtained from the heart tissue repositories at the University of Pittsburgh and the University of Colorado Health Sciences Campus as described previously.[21,25,26]

**MASS SPECTROMETRY: $BAG3^{+/+}$ (WT) AND $BAG3^{+/-}$ MICE.** LV tissue from three WT and three $Bag3^{+/-}$ mice were homogenized in a lysis buffer containing 9 M urea and then briefly sonicated. The homogenate was then centrifuged at 10,000 relative centrifugal force for 10 minutes and the supernatant containing the solubilized protein was collected. Protein concentration was determined by bicinchoninic acid assay (Pierce). Approximately 300 μg of protein from each sample were used for proteomics. A detailed description of the methodology used for separation of the proteins is provided in the Supplemental Appendix.

The raw mass spectrometry data were imported into the Peaks Bioinformatics software and searched against the *Mus musculus* database with carbamidomethylated cysteine as the fixed modification and phosphorylation as the variable modification. The data were analyzed using the built-in label-free quantification option normalized to the total ion current of each sample. Proteins of interest identified by this method were further examined by pathway analysis using the DAVID bioinformatics program (Database for Annotation, Visualization and Integrated Discovery, version 6.8), which allowed for protein function and cell compartment characterization.[27,28]

**TERMINAL DEOXYNUCLEOTIDYL TRANSFERASE DEOXYURIDINE TRIPHOSPHATE NICK END LABELING STAINING FOR CELL DEATH.** Isolated adult mouse cardiomyocytes were plated on Lab-TekII Chamber Slide system coated with laminin. Cells were subjected to hypoxia (1 hour) and reoxygenation (2 hours) before staining with 100 nM Nonyl Acridine Orange (Molecular Probes Cat# A1372) in Tyrode's buffer for 30 minutes. Cells were then labeled with TMR red (Roche TMR red in situ cell death detection kit) and

imaged by confocal microscopy as previously described.[29]

**TMRM STAIN FOR MITOCHONDRIAL MEMBRANE POTENTIAL AND MITOCHONDRIA CONTENT.** Isolated adult mouse cardiomyocytes were plated as described in the terminal deoxynucleotidyl transferase deoxyuridine triphosphate nick end labeling (TUNEL) staining section. Cells were stained with 100 nM tetramethylrhodamine, methyl ester, perchlorate (TMRM) (Thermo Fisher Scientific Cat# T668) in Tyrode's buffer. Imaging was performed as described previously by confocal microscopy.

**MitoSOX STAINING FOR MITOCHONDRIAL REACTIVE OXYGEN SPECIES CONTENT.** Isolated adult mouse cardiomyocytes were plated as described in the TUNEL staining section. Cells were stained with 5 μM MitoSOX Red Mitochondrial Superoxide Indicator (Thermo Fisher Scientific Cat# M36008) and confocal images were quantified in Fiji Image J.

**PREPARATION NEONATAL RAT VENTRICULAR CARDIOMYOCYTES.** Neonatal rat ventricular cardiomyocytes (NRVC) were prepared as described previously and were generously provided by Walter J. Koch, PhD, and Jessica Ibetti, PhD.[30]

**ISOLATION AND CULTURE OF ADULT MYOCYTES.** Adult cardiac myocytes were isolated form the septum and LV free wall of $Bag3^{+/+}$ (WT), $Bag3^{-/-}$, and $Bag3^{+/-}$ mice , plated on laminin-coated glass coverslips, and then handled as first described by Zhou et al[31] with later published modifications by members of this research team.[32-34]

**BAG3 KNOCKDOWN.** NRVCs at 60% to 70% confluence were transfected using the lipofectamine RNAiMAX Kit (Invitrogen) with a Bag3-specific small interfering RNA (siRNA) according to manufacturer's instructions for 72 hours.

**HYPOXIA/REOXYGENATION.** NMVCs were subjected to hypoxia/reoxygenation as described previously.[29,30] In brief, NMVCs were exposed to humidified 5% $CO_2$:95% $N_2$ for 16 hours at 37°C and incubated in glucose-free medium. Cells were then reoxygenated with 5% $CO_2$:95% humidified air for 4 hours in medium containing glucose.

**CELL HARVEST AND PROTEIN EXTRACTION.** Cultured cells were washed in 1× PBS and lysed in lysis buffer supplemented with mammalian protease inhibitor cocktail and then scraped from the dish. Cells were sonicated and then centrifuged at 13,000 × g for 5 minutes in the cold. The supernatant was collected and used for protein analysis.[34,35]

**PROTEIN ISOLATION.** Hearts were excised, the left ventricles were separated and flash frozen in liquid nitrogen and stored at ⁻80°C until use. Membrane proteins were prepared as described previously using a Bullet Blender (Next Advance).[33]

**CYTOPLASMIC AND MITOCHONDRIAL FRACTIONATION.** Mitochondrial and cytoplasmic proteins were separated using a Mitochondria Isolation Kit for Cultured Cells (ThermoFisher, #89874) following instructions from the manufacturer.

Isolated protein was quantified using the Braford assay (Bio-Rad). Proteins were then separated by western blot analysis.

**IMMUNOPRECIPITATION.** NRVCs or AC16 cardiomyocytes were plated onto a 10-cm dish and treated as described above. Cells were quickly washed with cold phosphate-buffered saline (PBS) solution and placed into IP lysis buffer (ThermoFisher) that was supplemented with phosphatase inhibitor and halt proteinase inhibitor and sonicated. The protein were incubated with Magna magnetic beads (A/G) (Millipore, Sigma) primary antibody overnight as described previously.[19]

**WESTERN BLOT ANALYSIS.** Protein lysate (20 μL) was mixed with a reducing agent (Thermo Fisher) and proteins were separated using a Bolt 4% to 12% Bis-Tris Gel (Invitrogen) transferred to nitrocellulose membranes (LI-COR) by using a wet transfer system as we have described previously.[19] Membranes were quickly washed, blocked with LI-COR Odyssey blocking buffer and incubated with the primary antibodies overnight. The secondary antibody was incubated for 1 to 2 hours and resulting images were captured with a LI-COR imaging system. All primary antibodies and second antibodies are listed in the Supplemental Appendix.

**IMMUNOFLUORESCENT STAINING.** Neonatal or adult cardiomyocytes were fixed with 4% paraformaldehyde in PBS for 15 minutes then washed, permeabilized with 0.5% Triton X-100 in PBS for 10 minutes then washed and blocked with LI-COR blocking buffer S containing 5% bovine serum albumin and 0.1% Triton X-100 for 1 hour, all at room temperature. The cells were incubated overnight at 4°C with rabbit anti-protein of interest antibody diluted in blocking solution. Cells were then washed with PBS and incubated for 45 minutes at room temperature with suitable secondary antibody and 4′,6-diamidino-2-phenylindole (DAPI) diluted in blocking solution.

JACC: BASIC TO TRANSLATIONAL SCIENCE VOL. 8, NO. 7, 2023
JULY 2023:820–839

**CONFOCAL MICROSCOPY.** Confocal microscopy was used in adult cardiomyocytes as described previously.[19,29] Bag3 was identified using a primary rabbit antibody (1:200; Proteintech Group, Inc). Antibodies for proteins of interest were as described in the Supplemental Appendix, including identification of antibodies and their suppliers and catalogue numbers.

Total laser intensity and photomultiplier gain were set at constant for all groups, and settings and data were verified by 2 independent observers who were blinded to the experimental group. A minimum of 3 coverslips were used for each experimental group, and at least 3 cell images were acquired from each coverslip.

**MEASUREMENT OF MITOCHONDRIAL MEMBRANE POTENTIAL AND MITOCHONDRIAL $CA^{2+}$ UPTAKE.** Measurements were made as we have described previously. A full description of the method is found in the Supplemental Appendix. In brief, LV myocytes isolated from WT and $Bag3^{+/-}$ hearts were exposed to either 21% $O_2$-5% $CO_2$ (normoxia) or 1% $O_2$-5% $CO_2$ (hypoxia) for 30 minutes followed by 30 minutes of reoxygenation.[32] Permeabilized myocytes were supplemented with succinate. Fura-FF (0.5 μM) was added at 0 seconds and JC-1 (800 nM; Molecular Probes) at 20 seconds to measure extramitochondrial $Ca^{2+}$ and mitochondrial membrane potential ($\Delta\Psi_m$), respectively.

Fluorescence signals were monitored with multiwavelength-excitation and a dual wavelength-emission spectrofluorometer (Delta RAM, Photon Technology International). The ratiometric dye Fura-FF was calibrated as previously described.[36,37] At times indicated, 10 μM $Ca^{2+}$ pulse was added and $\Delta\Psi_m$ and extramitochondrial $Ca^{2+}$ were monitored simultaneously. $\Delta\Psi_m$ was calculated as the ratio of the fluorescence of the JC-1 oligomeric to monomeric forms.

Cytosolic $Ca^{2+}$ clearance rate was taken to represent mitochondrial $Ca^{2+}$ uptake.

**ECHOCARDIOGRAPHY.** Global LV function was evaluated in all mice after light sedation (2% isoflurane) using a VisualSonics Vevo 770 imaging system and a 707 scan head as described previously.[12] The left ventricular ejection fraction was calculated by measuring the left ventricular internal diameter end diastole and the left ventricular internal diameter end systole. These measurements were facilitated using the Vevo 770 system which provides highly visible systolic and diastolic endocardial surfaces.

**MEASUREMENT OF MITOCHONDRIAL $CA^{2+}$ UNIPORTER CURRENT.** Myocytes were isolated from LV and septum of 8- to 12-week-old WT or $BAG3^{+/-}$ mice.[12] Myocytes were then infected with Adv-GFP or Adv-Bag3 ($7 \times 10^6$ pfu/mL) and cultured for 24 hours before use for mitoplast isolation.[32,33] Mitoplast patch clamp recordings were conducted at 30°C as previously described in detail and in the Supplemental Appendix.[34-36] The mitochondrial $Ca^{2+}$ uniporter (MCU) current ($I_{MCU}$) was recorded using a computer controlled Axon200B patch-clamp amplifier with a Digidata 1320A acquisition board (pClamp 10.0 software; Axon Instruments). Mitoplasts were bathed in physiologic solutions and after formation of GΩ seals mitoplasts were ruptured, and capacitance was measured. After capacitance compensation, mitoplasts were held at 0 mV and $I_{MCU}$ was elicited with a voltage ramp (from $^-$160 mV to $^+$80 mV, 120 mV/s) both before and after addition of 5 mM Ca. A full description of the methods is found in the Supplemental Appendix.[37-40]

**STATISTICAL ANALYSIS.** Data are presented as mean ± SEM for continuous variables. One-way analysis of variance (ANOVA) with Bonferroni post hoc test was used for multiple comparisons. The data was evaluated for normality to assure that parametric statistics could be used. Within and between group comparisons were performed with paired and unpaired Student *t* tests, respectively. For western blot analysis, $P < 0.05$ was considered significant. The control for each experiment (eg, Ad-GFP or normoxia) was set as 1.0. The full blots used for assessment of protein levels including the loading standard are shown for each experiment and each experiment was replicated at least once and achieved comparable results. All blots were normalized by the appropriate standard from the same gel which is found below each investigational western. Individual elements on each figure represent a distinct biological measurement in 1 sample from a single mouse. No technical replicates are observed in the result sections of this study unless noted. The original blot for each figure is available upon request from verifiable scientists. In the case of measurement of the levels of the multiple components of the uniporter, each experiment was repeated 5 times because of the small protein yield in each experiment. A commercially available software package (JMP version 12, SAS Institute) was used for statistical analysis.

## RESULTS

**CARDIOMYOCYTE-RESTRICTED BAG3 HAPLOINSUFFICIENCY IS ASSOCIATED WITH ALTERED MITOCHONDRIAL PROTEIN EXPRESSION IN YOUNG MICE.** $Bag3^{+/-}$ mice provide an ideal model in which to study the biology of Bag3 because they mirror the phenotype of Bag3 deletions

**FIGURE 1** **Cardiomyocyte-Specific Bag3 KO Disrupts Expression of Mitochondrial Proteins Involved in Cell Metabolism and Apoptosis**

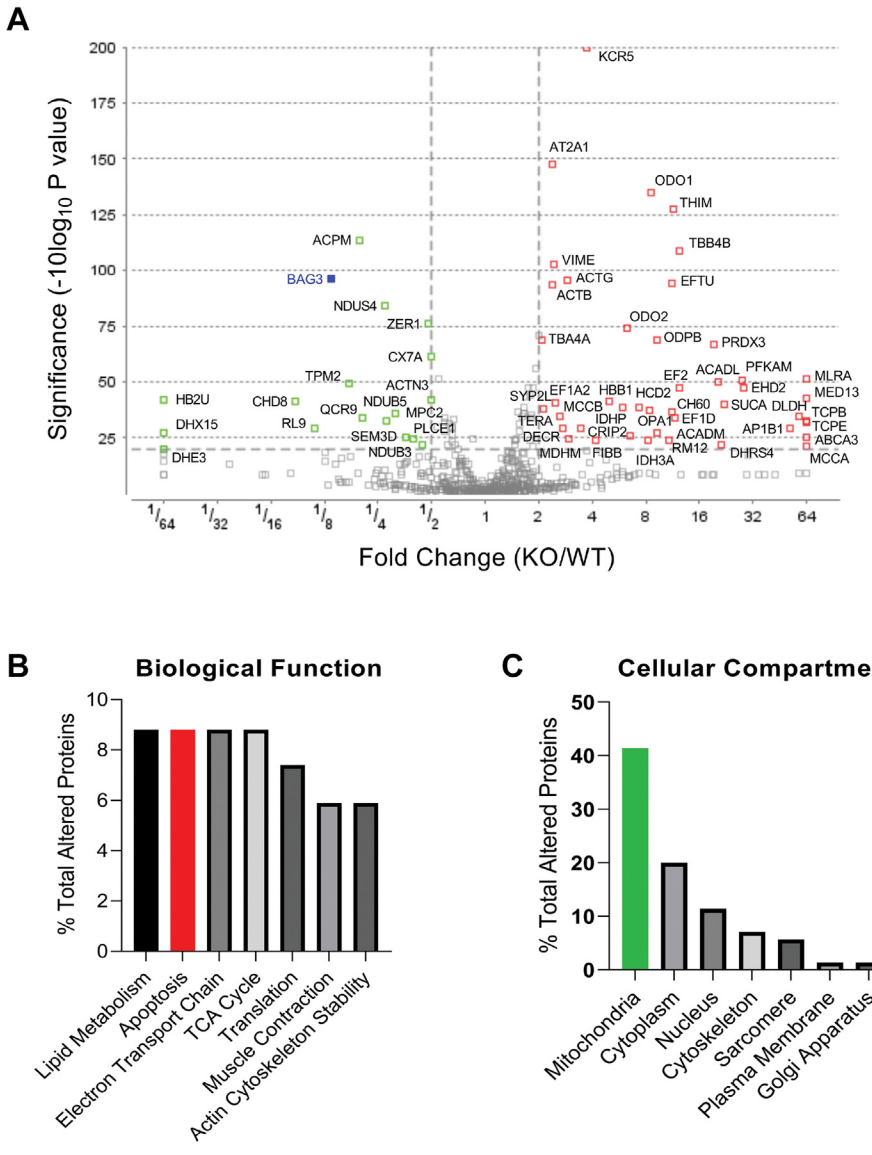


**(A)** Volcano plot analysis of all proteins from the wild-type (WT) and Bcl2-associated athanogene-3 ($Bag3^{+/-}$) mouse left ventricle identified by bottom-up mass spectrometry. Significance cutoff is set to $P = 0.05$. **Green** indicates decreased expression compared with WT. **Red** indicates increased expression (n = 3 WT, 3 $Bag3^{+/-}$). **(B)** Graphical summary of the proteins with altered expression in the $Bag3^{+/-}$ mice grouped by their biological function(s). **(C)** Graphical summary of the proteins with altered expression the Bag3 knockout (KO) mice grouped by their primary cellular compartment. Biological function and cellular component information were obtained using the DAVID bioinformatics program (Database for Annotation, Visualization and Integrated Discovery, version 6.8). TCA = tricarboxylic acid.

or truncations in that the ventricle dilates progressively over time, beginning in mice at 10 to 12 weeks of age whereas 8- to 10-week-old $Bag3^{+/-}$ mice have a normal phenotype by echocardiography (Supplemental Figure 1). To gain an insight into which specific pathways are dysregulated when Bag3 expression is reduced by 50% but before phenotypic changes characteristic of HFrEF are evident, we used unbiased mass spectrometry to analyze the proteome of young $Bag3^{+/-}$ mice compared to age-matched WTcontrols.[11,12]

Proteins from the mouse left ventricle subjected to high pressure liquid chromatography coupled to tandem mass spectrometry followed by label-free

JACC: BASIC TO TRANSLATIONAL SCIENCE VOL. 8, NO. 7, 2023
JULY 2023:820–839

quantification (normalized by total ion current) analysis identified 86 proteins with significantly altered expression in the Bag3$^{+/-}$ mice ($P < 0.05$ vs WT) (**Figure 1A,** Supplemental Table 1).

Notably, when we conducted pathway analysis of these proteins, we found that the largest proportion (36%) are primarily localized in mitochondria (**Figure 1C**), suggesting that disruption of mitochondrial function may contribute to the cardiac dysfunction associated with reduced Bag3 expression. When we analyzed the 86 proteins by their biological function, we found that among their primary functions were regulating mitochondrial metabolism and mitochondria-dependent apoptosis (**Figure 1B**).

**THE STRESS OF HYPOXIA/REOXYGENATION: APOPTOSIS IN BAG3$^{+/-}$ MICE.** To determine how haploinsufficiency of Bag3 might influence apoptosis, we harvested adult myocytes from 8- to 10-week-old WT and Bag3$^{+/-}$ mice, stained them for nuclear DNA (DAPI), viable mitochondria (nonyl acridine orange [NAO]) and damaged DNA (TMR Red-TUNEL), and analyzed the resulting confocal images (**Figure 2A**) with ANOVA followed by subgroup analysis with Bonferroni correction (**Figure 2B**) ($P < 0.013$ is statistically significant). In the absence of stress, there was a very small but nonsignificant ($P = 0.11$) increase in apoptosis in the Bag3$^{+/-}$ mice. When WT myocytes were stressed with 1 hour of hypoxia and subsequent reoxygenation (H/R) for 2 hours, there were significantly ($P < 0.001$) more TUNEL-positive cells when compared to WT-normoxic cells. Similarly, H/R resulted in significantly ($P < 0.0001$) more TUNEL-positive Bag3$^{+/-}$ myocytes when compared to Bag3$^{+/-}$-normoxic cells. More interestingly, H/R resulted in significantly ($P = 0.08$) more TUNEL-positive cells in Bag3$^{+/-}$ myocytes when compared to WT-H/R myocytes; indicating that Bag3 haploinsufficiency exacerbates H/R injury.[42]

**HOMOZYGOUS LOSS OF BAG3 ALTERS $\Delta\Psi_m$.** A separate group of experiments was undertaken to measure the effects of Bag3 deletion on mitochondrial area (size) and the level of reactive oxygen species (ROS). Because pilot experiments suggested that heterozygous Bag3 deletion had no effect on mitochondrial ROS, we used cells isolated from Bag3$^{-/-}$ mice for these experiments but planned to follow-up positive studies. As seen in **Figure 2C**, homozygous deletion had no effect on mitochondrial ROS, nor did it have an effect on mitochondrial content (**Figure 2D**, right panel). By contrast, we found a significant ($P < 0.01$) decrease in the $\Delta\Psi_m$ in Bag3$^{-/-}$ mice when compared with WT mice (**Figure 2D**, left panel).

**COMPARATIVE ANALYSIS OF RELEVANT PROTEIN LEVELS IN BAG3$^{+/-}$ AND Bag3$^{WT}$ MICE.** We next sought to confirm the results of the proteomic studies by measuring the levels of proteins that are critical for myocyte homeostasis and proteostasis in LV myocardium of the Bag3$^{WT}$ and Bag3$^{+/-}$ mice with a focus on apoptosis-related proteins. As seen in **Figure 3A**, there was a significant ($P < 0.01$) increase in the levels of caspase-3, a primary executioner (effector) protein of apoptosis.[43] However, the ratio of cleaved caspase-3/total caspase-3 protein was not elevated in the ventricular myocardium from Bag3$^{+/-}$ mice when compared with protein isolated from the hearts of WT mice suggesting that Bag3 haploinsufficiency causes only modest to minimal apoptosis at the early stage of the disease. We hypothesized that, although we did not observe activation of caspase-3 with early disease when cardiac remodeling was absent, we might see activation of caspase-3 in older mice with cardiac remodeling and diminished function.[44] However, when we looked at older mice at either 10 to 12 weeks of age or at 18 to 22 weeks of age, the ratio of cleaved caspase-3/total caspase-3 protein still was not increased (compared to WT) suggesting the possibility that only profound stress coupled with old age would activate caspase-3-mediated apoptosis in the murine heart (**Figure 3B**).

**BAG3 DEFICIENCY AND THE EXTRINSIC PATHWAY OF APOPTOSIS.** We next sought to evaluate the extrinsic/mitochondrial independent apoptosis pathway that is activated by tumor necrosis factor (TNF)-α through binding to the TNFR1 receptor with the subsequent cleavage and activation of caspase-8.[45] Cleaved caspase-8 can then activate caspase-3 which leads directly to apoptosis and to the release of cytochrome c. The extrinsic pathway was clearly activated in the Bag3$^{+/-}$ mice as levels of TNF-α were significantly higher in Bag3$^{+/-}$ mice ($58.0 \pm 2.7$, $n = 5$; $P = 0.014$) when compared with WT littermate control mice ($36.7 \pm 2.7$; $n = 5$) (**Figure 3C**). These effects were TNF-restricted as we could not demonstrate any change in the levels of proinflammatory cytokine IL-6 (**Figure 3C**). The role of extrinsic signaling in apoptosis in Bag3$^{+/-}$ mice was further supported by the finding that the ratio of cleaved caspase-8/total caspase-8 ($0.94 \pm 0.09$, $n = 5$) was significantly ($P < 0.003$) increased in Bag3$^{+/-}$ ventricular myocardium when compared with tissue obtained from WT mice ($0.54 \pm 0.03$, $n = 5$) (**Figure 3D**).[43]

That the decrease in the levels of Bag3 was associated with an increase in cellular inflammation was supported by the finding that Bag3$^{+/-}$ hearts had a significant increase of poly(ADP-ribose) polymerase

**FIGURE 2 TUNEL-Positive Cells Are Higher but Mitochondrial Membrane Potential Are Lower in Bag3$^{+/-}$ Mice Subjected to Hypoxia/Reoxygenation**

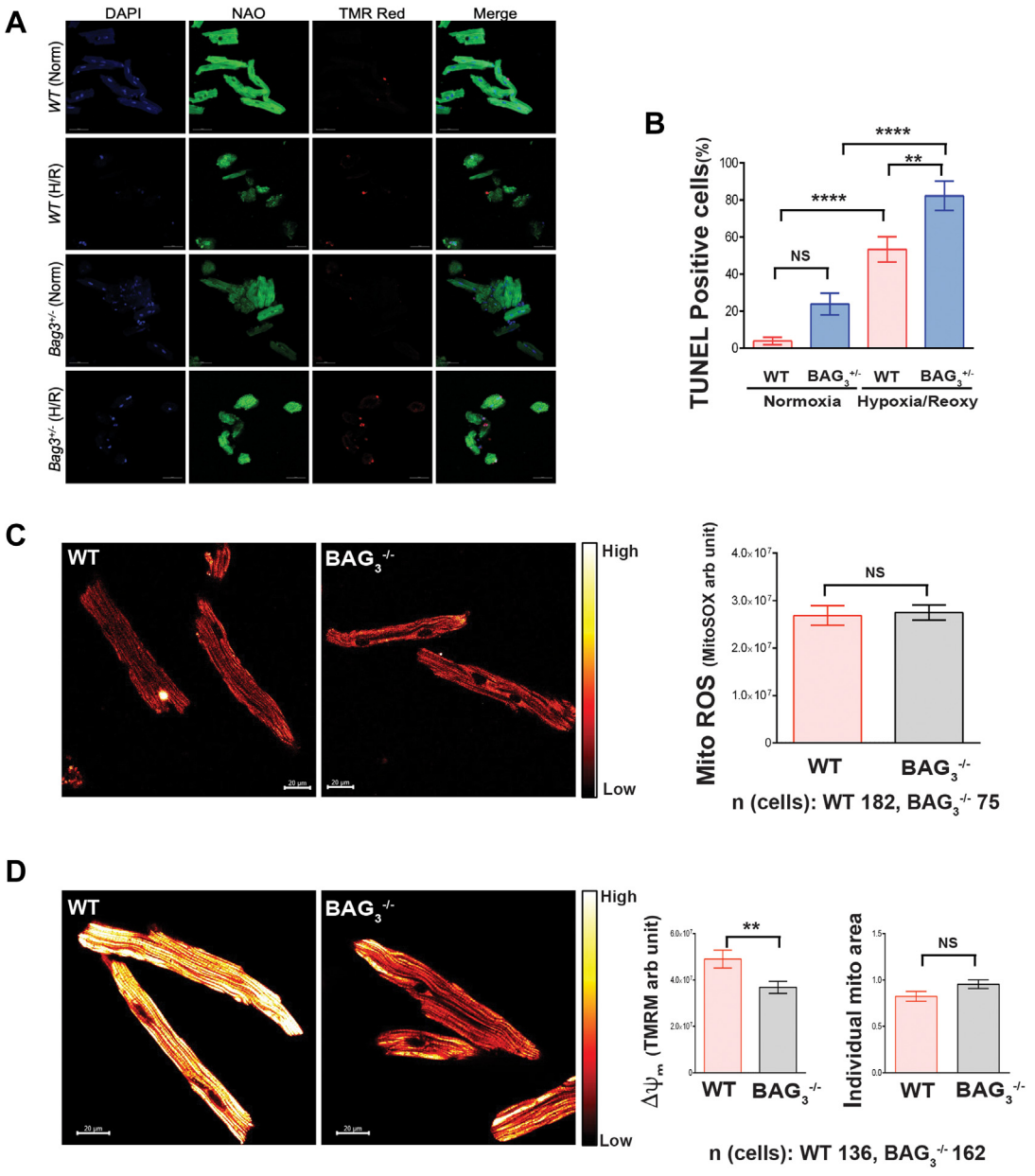


**(A, B)** Terminal deoxynucleotidyl transferase deoxyuridine triphosphate nick end labeling **(**TUNEL) staining. Adult mouse cardiomyocytes isolated from WT and Bag3$^{+/-}$ mice were subjected to hypoxia/reoxygenation (H/R) as well as normoxia (Norm) control conditions. Cells were stained with nonyl acridine orange (NAO), TMR red, and DAPI before imaging with a Zeiss LSM 900 confocal microscope. Statistical significance was determined using 1-way analysis of variance (ANOVA) with Bonferroni correction for multiple subcomparisons. ****$P < 0.0001$. **$P < 0.01$ (n = 10 images per group). Scale bar = 50 μm. **(C)** MitoSOX staining. Adult mouse cardiomyocytes isolated from WT and Bag3$^{-/-}$ mice were stained with MitoSOX and imaged with a Zeiss LSM 900 confocal microscope. MitoSOX fluorescence was quantified using the Fiji Image J, and data are plotted in GraphPad Prism 7 software. Representative images are shown with WT on the left and Bag3$^{-/-}$ on the right. Statistical significance was determined using the Student *t* test (n = 75 to 182 cells per group). Scale bar = 20 μm. **(D)** TMRM staining. Adult mouse cardiomyocytes isolated from WT and Bag3$^{-/-}$ mice were stained with TMRM and imaged with a Zeiss LSM 900 confocal microscope. TMRM fluorescence was quantified using the Fiji Image J, and data were plotted in GraphPad Prism 7 software. Representative images from WT mice on the **left** and Bag3$^{-/-}$ on the **right**. Mitochondrial content is quantified as individual mitochondria area using Mito-Morphology Image J. Data are presented as the mean ± SEM. Statistical significance was determined using a Student *t* test. **$P < 0.01$ (n = 136 to 162 cells per group). Scale bar = 20 μm. NS = not significant; ROS = reactive oxygen species; other abbreviation as in Figure 1.

**FIGURE 3 Western Blot Analysis of Proteins Involved in Mitochondrial Dependent or Mitochondrial Independent Apoptotic Signaling in Both Young and Old Bag3$^{+/-}$ and Bag3$^{WT}$ Mice**

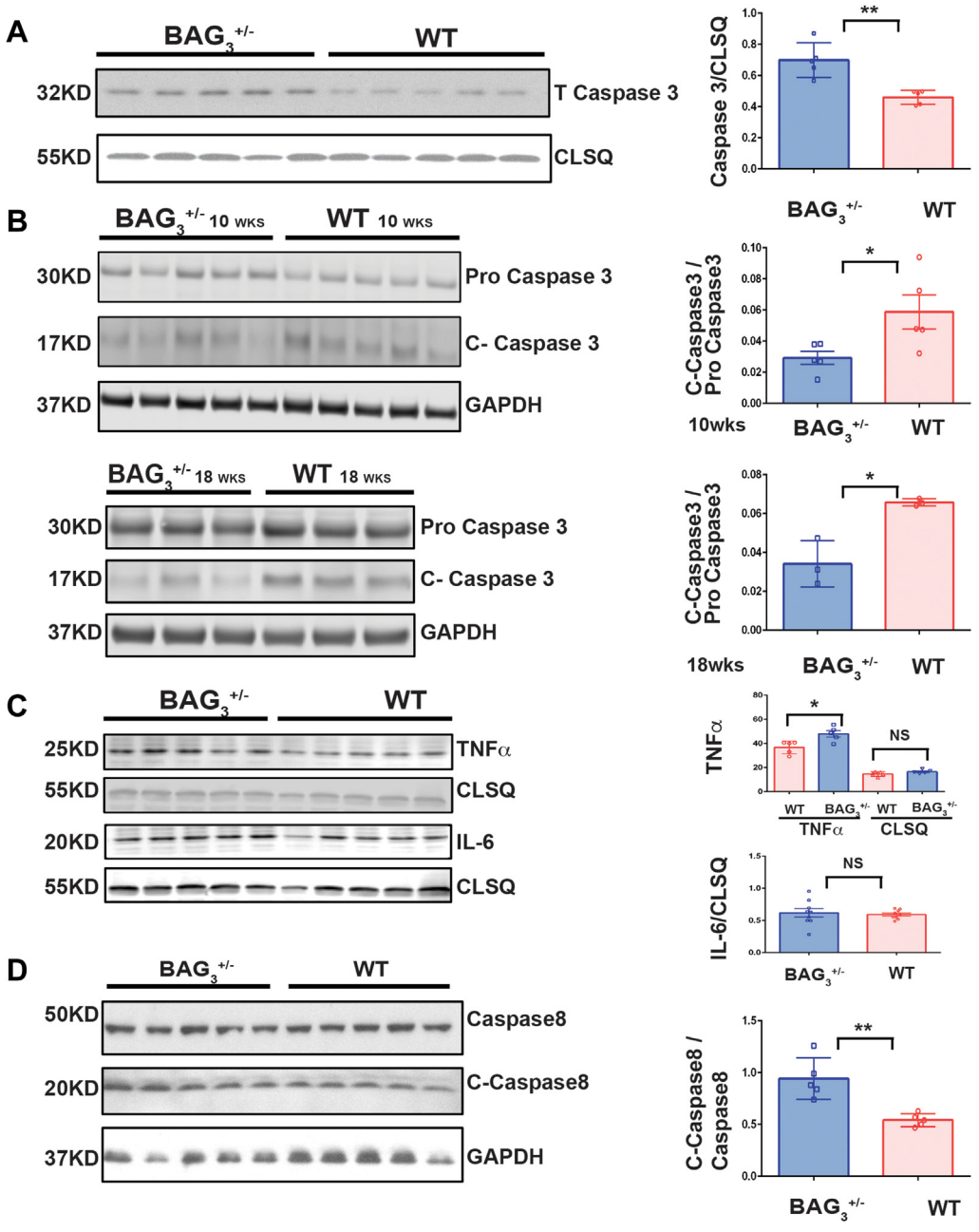


The data shown in the individual bar graphs are derived from the accompanying western blots. n = 5 in each experimental group, with the exception of the samples obtained from the older (18 week) mice in **B** where the sample size was 3 per investigational group. Each experiment was repeated at least once with tissue obtained from the same mice or identically aged mice. All data are presented as the mean ± SEM. *$P < 0.05$. **$P < 0.01$. **(A)** Levels of total caspase-3 are significantly higher in Bag3$^{+/-}$ mice than in Bag3$^{WT}$ mice. However, as seen in **B**, the ratio of cleaved caspase-3 to pro caspase-3 in tissue from Bag3$^{WT}$ mice was higher than in Bag3$^{+/-}$ mice and the same was true in older 18-week-old mice despite the fact that left ventricular ejection fraction (LVEF) was significantly diminished and left ventricular (LV) dilatation was obvious in the older mice (See also Supplemental Figure 1). **(C)** Levels of tumor necrosis factor alpha (TNFα) are significantly elevated in Bag3$^{+/-}$ mice; however, there is no change in levels of interleukin (IL)-6, suggesting that the cytokine effect is highly specific. **(D)** By contrast with caspase-3, there was a significant ($P < 0.01$) increase in levels of cleaved caspase-8 divided by total caspase-8, suggesting that caspase-8 was activated in mice with no obvious heart failure phenotype. CLSQ = calseqestrin; GADPH = glyceraldehyde-3-phosphate dehydrogenase; other abbreviations as in **Figure 1**.

**FIGURE 4** **Measurement of the Levels of Cardiac Proteins in Murine Hearts With Bag3 Haploinsufficiency (Bag3$^{+/-}$) or in Nontransgenic WT Littermate Controls and the Presence or Absence of Myofibrillar Disarray**

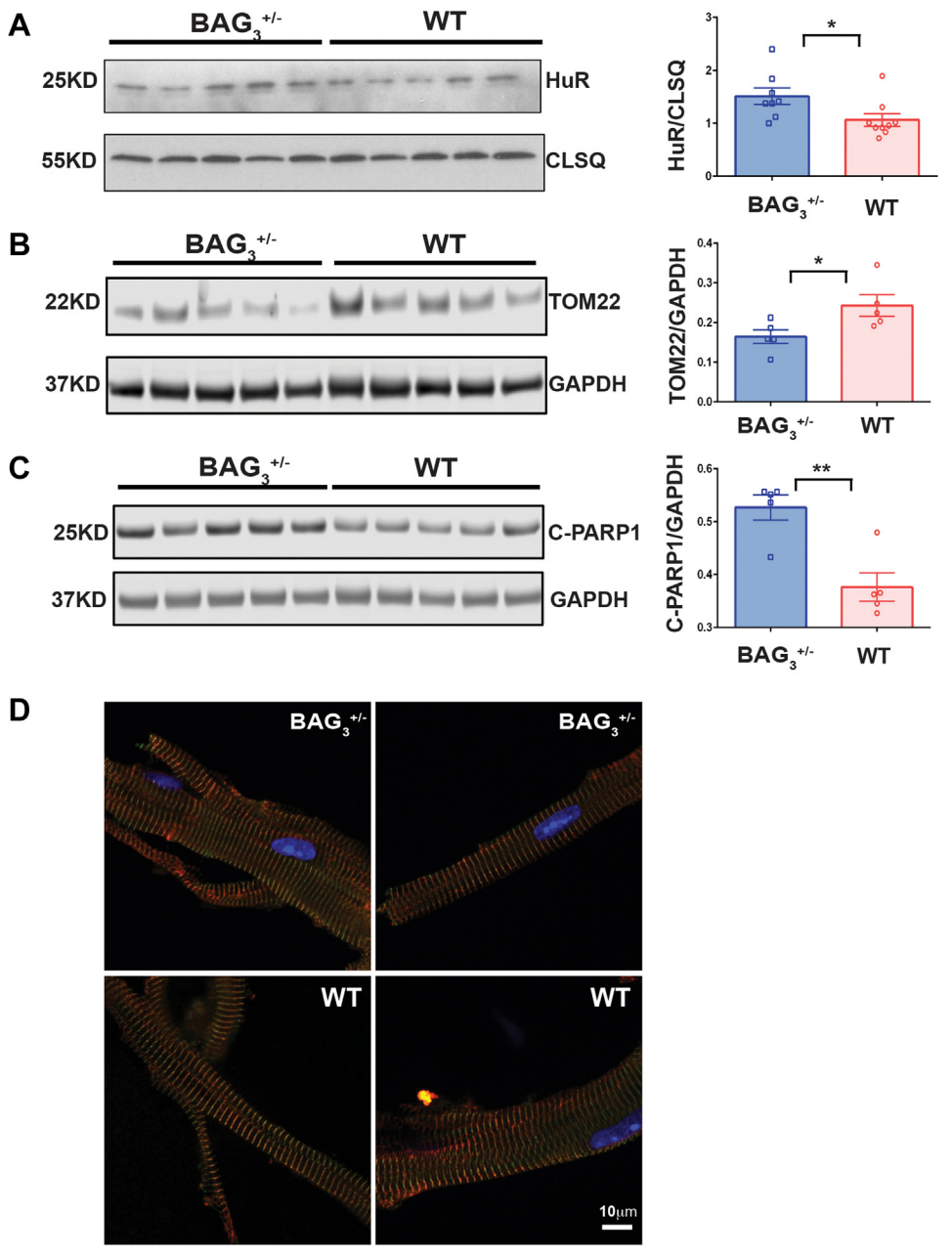


Representative western blots of proteins isolated from tissue derived from young Bag3$^{+/-}$ or WT mice before development of characteristic changes in the morphologic phenotype seen characteristically in older Bag3$^{+/-}$ mice. The data shown in the individual bar graphs are derived from the accompanying western blots (n = in each experimental group). All mice are 8 to 10 weeks old with normal left ventricular size and function. **(A to C)** Human receptor R (HuR) **(A)** and C-PARP1 **(C)** levels were elevated, but TOM22 levels **(B)** were reduced in Bag3$^{+/-}$ hearts. The data are presented as mean ± SEM. Each experiment was repeated at least once with comparable results. *$P < 0.05$. **$P < 0.01$. **(D)** No sarcomere disarray was observed in 6-week-old Bag3$^{+/-}$ mice. Immunofluorescence image of WT **(lower panel)** and Bag3$^{+/-}$ **(upper panel)** cardiomyocytes immunostained for α-actinin **(green)** and Bag3 **(red)**. Original magnification ×63. Scale bars = 10 μm. The image is representative of the 5/group acquired. The experiment was repeated once with comparable results. C-PARP1 = cleaved PARP1; other abbreviations as in Figures 1, 3, and 4.

**FIGURE 5 Investigating the Role of cIAP and SMAC in Bag3-Mediated Autophagy**

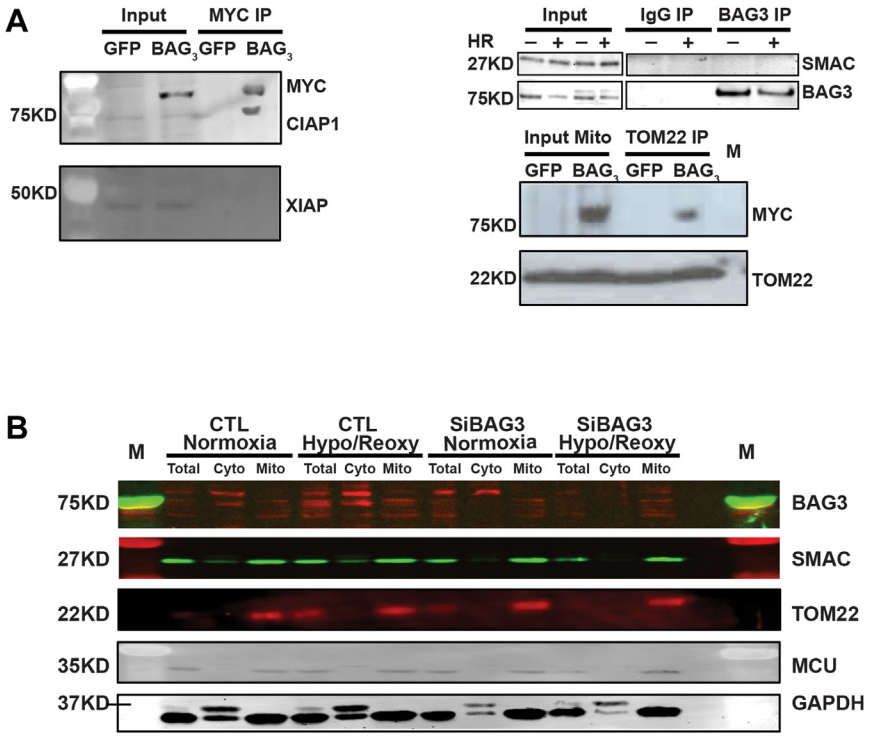


Two proteins that are thought to play a role in modulating apoptosis are second mitochondria-derived activator of caspase (SMAC) and cellular inhibitor of apoptosis (cIAP). However, as seen in Supplemental Figure 3, their levels are not changed in hearts of young Bag3$^{+/-}$ mice despite the observation of an increase in activated caspase 8 (Figure 3). To better understand the role of cIAP1 and SMAC, we undertook 2 experiments. **(A)** Coimmunoprecipitation studies identify Bag3 partners. From left to right: Bag3 bound the inhibitor of apoptosis protein (cIAP) but not the homologous XIAP. Bag3 also interacts with the mitochondrial membrane transport protein TOM22 but not with SMAC, a mitochondrial protein that translocates to the cytoplasm to support apoptosis by replacing cIAP on noncleaved caspases. **(B)** The effects of the stress of hypoxia on the translocation of SMAC in the presence and absence of Bag3. Neonatal rat ventricular cardiomyocytes (NRVCs) were isolated and cultured under normoxic conditions, in the presence of small interfering RNA (siRNA) for Bag3 or scrambled control for 3 days. NRVCs were then subjected to 16 hours of hypoxia (1% $O_2$:5% $CO_2$) and 4 hours of reoxygenation (21% $O_2$:5% $CO_2$), or 20 hours of normoxia before cell fractionation studies. TOM22 (mitochondria), MCU (mitochondria), and GAPDH (cytoplasm) were used as controls to show that separation of the mitochondria had been accomplished. Bag3 was expressed to a greater degree in the cytoplasm of H/R-stressed myocytes but was absent or nearly absent in cells subjected to Bag3 knockdown by siRNA. SMAC was present in both the cytoplasm and the mitochondria; however, it was not obvious in the cytoplasm when Bag3 was ablated with siRNA. TOM22 was also found exclusively in the mitochondria. CTL = cytotoxic t lymphocytes; GFP = green fluorescent protein; IgG = immunoglobulin G; IP = immunoprecipitation; MCU = mitochondrial calcium uniporter; MYC = myelocytomatosis; other abbreviations as in Figures 2 and 3.

(PARP)-1 (Figure 4C), a protein that transfers ADP-ribose to apoptosis-inducing factor, resulting in its translocation from mitochondria to the nucleus where it initiates cell death by signaling DNA fragmentation.[39,45] Thus, in aggregate, our studies of protein levels in myocardial cells from mice in which 1 allele of Bag3 was deleted strongly suggest that canonical TNF-receptor signaling is a characteristic feature of Bag3 haploinsufficiency and that it leads to the activation of PARP-1, which in turn results in sterile inflammation and DNA fragmentation.[39,45]

**CASPASES, SMAC, AND cIAP: CONTROL OF APOPTOTIC SIGNALING.** Our data in the young Bag3$^{+/-}$ mice presented a conundrum: how could apoptosis be clearly increased in adult myocytes from Bag3$^{+/-}$ mice if the ratios of cleaved/pro caspase-3 were unchanged? A possible explanation for this discrepancy is potential changes in the function of second mitochondria-derived activator of caspase (SMAC), a protein transcribed by the *DIABLO* gene that is located in the intermitochondrial space. As seen in Figure 5A, we show for the first time that

cellular inhibitor of apoptosis (cIAP) co-immunoprecipitates (co-IPs) with Bag3 and that Bag3 co-IPs with cIAP but not with SMAC. We also show that the relationship between Bag3 and cIAP is selective as Bag3 does not co-IP with the highly homologous XIAP (x-linked IAP) (**Figure 5A**). Interestingly, Bag3 also co-IPs with the mitochondrial protein TOM22 (**Figure 5A**). TOM22 (along with TOM20) is an accessory unit of the Translocator of Outer Membrane (TOM), a pore in the outer mitochondrial membrane (OMM) that transports short chains of proteins into the mitochondrial matrix.

**SMAC IS STUCK IN THE OMM IN THE ABSENCE OF BAG3.** Our hypothesis was that caspase-3 was not activated with Bag3 haploinsufficiency due to SMAC being stalled in the mitochondrial membrane and not relocalizing to the cytoplasm. To address this hypothesis, we isolated neonatal myocytes from WT rats and cultured them. The cells were then exposed to: 1) normal control conditions; 2) H/R; 3) siRNA for Bag3; or 4) H/R plus Bag3 siRNA. As seen in **Figure 5B**, under control culture conditions, SMAC was prominent in the mitochondria with a small amount of protein in the cytoplasm. The addition of H/R stress on its own did not change this localization of SMAC. However, in the absence of Bag3 (siRNA Bag3) there was no appreciable SMAC in the cytoplasm. Similarly, no SMAC was observed in the cytoplasm when cells lacking Bag3 (siBag3) were exposed to the stress of H/R. TOM22 served as a control because it is exclusively mitochondrial. It remained in the mitochondria throughout the 4 experimental conditions leading us to suggest that the translocation of SMAC requires Bag3.

**THE BAG3$^{+/-}$ PRE–HEART FAILURE PROTEOME.** To gain a broader understanding of how Bag3 depletion impacts apoptosis, we assessed other apoptotic signaling proteins that are associated with myocardial failure. We found no changes in the levels of Bcl2, a potent inhibitor of apoptosis that is a binding partner of Bag3 (Supplemental Figure 2). We also did not see changes in the levels of: 1) the cellular inhibitor of apoptosis – cIAP1 (Supplemental Figure 2B); 2) the mitogen-activated protein kinase P38 that mediates inflammation and apoptosis[46] (Supplemental Figure 2B); or 3) endonuclease G, a mitochondrial nuclease that translocates to the nucleus where it initiates DNA fragmentation. (Supplemental Figure 2C); or 4) SMAC, a mitochondrial protein that translocates to the cytoplasm where it activates caspases by competing with cIAP for the activation site (Supplemental Figure 2D). Similarly, we saw no changes in the levels of JNK (Supplemental Figure 3A), Jun (Supplemental Figure 3B), or ERK1/2 (Supplemental Figure 3C), all of which have been shown to be differentially regulated in the context of symptomatic HFrEF and are therefore part of the molecular phenotype of established HFrEF.

One observation from the proteomic screens that was unexpected but consistent with the overarching hypothesis was that abnormal levels of Bag3 led to an increase in the cardiac inflammasome even before the onset of changes in the traditional elements of the symptomatic (or echocardiographic) HFrEF proteome. The RNA-binding protein Human Antigen R (*ELAV-1*) was over-expressed in the Bag3$^{+/-}$ hearts ($1.51 \pm 0.16$, $n = 8$) when compared with levels in WT control mice ($1.07 \pm 0.11$, $n = 9$; $P = 0.03$) (**Figure 4A**).[47] We also found a significant increase in the levels of PARP1, an enzyme that functions in ADP ribosylation (**Figure 4C**) but a significant decrease in the levels of TOM 22, a protein that regulates the uptake of proteins and other nutrients into the mitochondrial matrix (**Figure 4B**).

A hallmark of HFrEF in both humans and in animal models has been the presence of myofibrillar disarray. Therefore, we wondered whether the marked differences in the phenotypes of young mice carrying a loss-of-function mutation in Bag3 would influence the structural aspects of cardiac myocytes. However, as seen in **Figure 4D**, there was no evidence of myofibrillar disarray.

**BAG3 HAPLOINSUFFICIENCY CAUSES ABNORMAL MITOCHONDRIAL CA$^{2+}$ HOMEOSTASIS.** Our proteomic studies have shown that a primary effect of Bag3 haploinsufficiency was a change in the amount of specific mitochondrial proteins that functioned in cellular metabolism and energy production (**Figures 1A to 1C**, Supplemental Table 1). Specifically, the knockout of 1 allele of Bag3 resulted in decreased expression of enzymes associated with mitochondrial function including isocitrate dehydrogenase, pyruvate dehydrogenase, and alpha ketoglutarate dehydrogenase. Therefore, we used 3 investigational approaches to test the hypothesis that haploinsufficiency of Bag3 could be a causative factor in the diminished function of Bag3$^{+/-}$ hearts because it led to abnormal mitochondrial $Ca^{2+}$ homeostasis.

**Haploinsufficiency of Bag3 impedes the ability of the heart to maintain the mitochondrial membrane potential.** In the first set of experiments, we extracted adult myocytes from WT and Bag3$^{+/-}$ mice. The myocytes were then exposed to H/R and $\Delta\Psi_m$ was evaluated using the ratiometric

**FIGURE 6** The Effects of Bag3 Haploinsufficiency on Mitochondrial Membrane Potential and $Ca^{2+}$ Uptake in Isolate Myocytes and in Mitoplasts From $Bag3^{+/-}$ and $Bag3^{WT}$ Mice

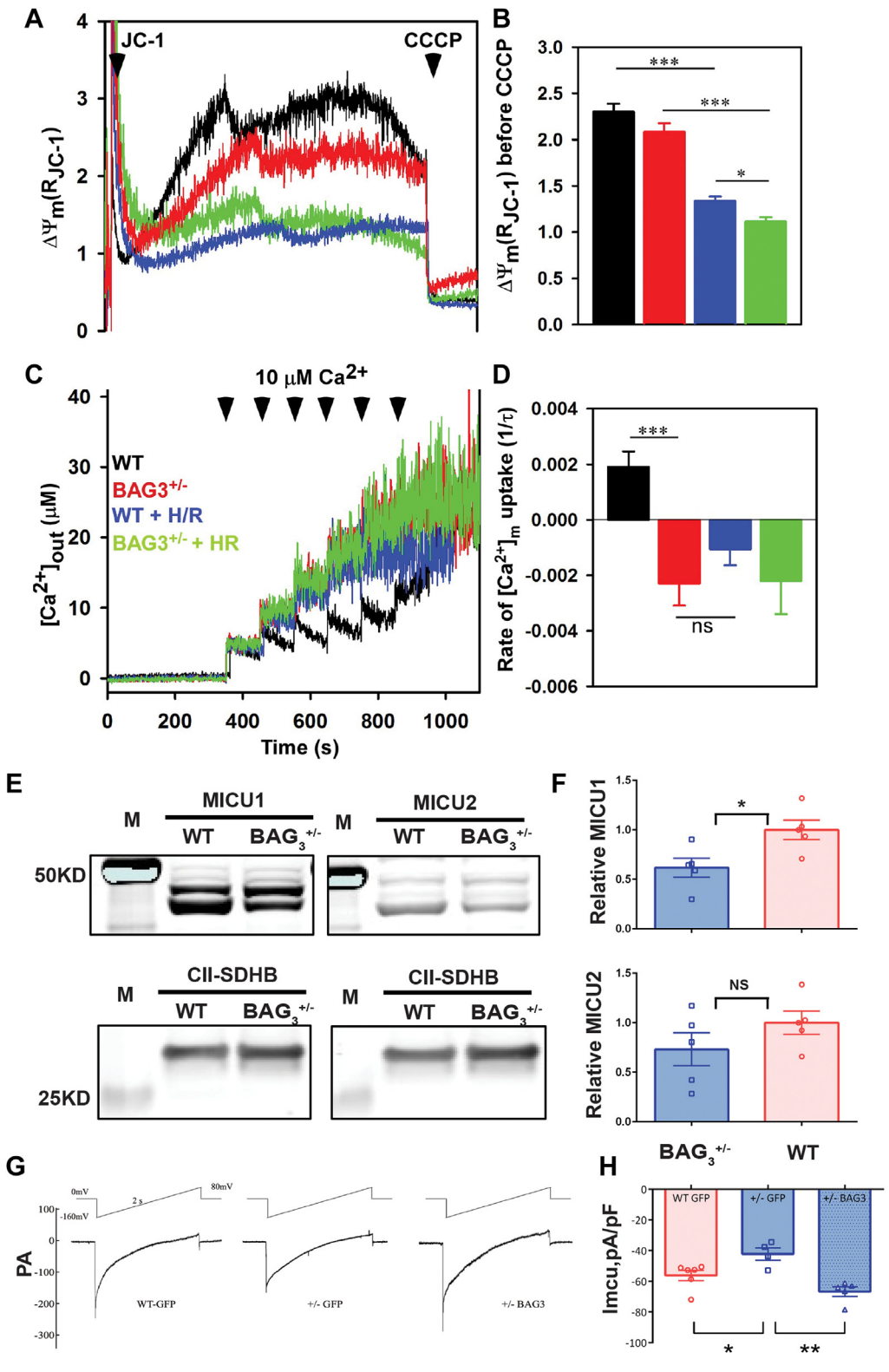


*Continued on the next page*

indicator JC-1 and mitochondrial $Ca^{2+}$ uptake using ratiometric dye Fura-FF.[48] There was a significant ($P < 0.001$) decrease in the $\Delta\Psi_m$ in myocytes from normoxic WT hearts when compared with myocytes from WT hearts that were exposed to the stress of H/R (Figures 6A and 6B). There was also a significant reduction ($P < 0.001$) in

$\Delta\Psi_m$ in myocytes from $Bag3^{+/-}$ mice when compared with myocytes from $Bag3^{+/-}$ mice after H/R. However, there was an additional significant ($P < 0.05$) reduction in $\Delta\Psi_m$ in $Bag3^{+/-}$ myocytes when compared with WT myocytes exposed to H/R, suggesting that the stress of H/R aggravated the underlying effects Bag3 haploinsufficiency on mitochondrial function. A similar phenomenon was observed when we looked at the effect of the deletion of 1 allele of Bag3 on calcium homeostasis (Figures 6C and 6D). When adult myocytes from WT mice were compared with cells isolated from $Bag3^{+/-}$ mice, there was a significant ($P < 0.001$) decrease in the rate of $[Ca^{2+}]_m$ uptake ($1/\tau$)) by $Bag3^{+/-}$ mitochondria when compared with mitochondria from WT mice. In aggregate, these results support the hypothesis that Bag3 depletion results in substantial changes in $Ca^{2+}$ homeostasis especially in cells that are stressed.

**Heterozygous deletion of Bag3 alters the function of the $Ca^{2+}$ uniporter.** The uniporter is composed of 2 pore-forming subunits (MCU and MCUb) and 3 regulatory subunits (MICU1, MICU2, and EMRE) which together maintain the negative potential of the OMM.[41] This negative potential across the OMM is responsible for the movement of valuable resources into the mitochondria. Under resting conditions, MICU1 and MICU2 dimerize and serve as gatekeepers for the MCU. The initiation of cytosolic $[Ca^{2+}]$ release into the mitochondria causes a conformational change in the protein complex by blocking MICU2-dependent inhibition of $Ca^{2+}$ movement. MICU1 activates the channel and stimulates $Ca^{2+}$ transport into the mitochondria. EMRE stabilizes the MCU-MICU1 complex which, in turn, fine tunes the level of $Ca^{2+}$ that can enter the mitochondria. There was a trend towards a decrease in the level of MICU2 in $Bag3^{+/-}$ mice when compared with Bag3-WT mice, but this trend did not reach statistical significance (Figures 6E and 6F). However, there was a significant ($P < 0.05$) decrease in the levels of MICU1 in $Bag3^{+/-}$ mice when compared with the WT controls, providing further support that Bag3 haploinsufficiency is directly associated with and causative of the development of abnormalities in mitochondrial $Ca^{2+}$ homeostasis.

**MCU function is normalized by adenovirus overexpression of Bag3.** To confirm that decreased mitochondrial calcium uptake was due to reduced MCU activity and was directly related to the haploinsufficiency in Bag3, we isolated cardiac mitoplasts from WT myocytes and from $Bag3^{+/-}$ myocytes (both overexpressing GFP as a control).[49] Currents ($I_{MCU}$) were measured from voltage-clamped mitoplasts before and after addition of 5 mM $Ca^{2+}$. These measurements, although technically challenging, allow comparisons of MCU activity between different groups of mitochondria by tightly controlling conditions of membrane potential, $Ca^{2+}$, and $H^+$ gradients. $I_{MCU}$ were recorded during a voltage ramp as indicated. Peak $I_{MCU}$ in WT-GFP mitoplasts was significantly ($P = 0.018$) higher than $Bag3^{+/-}$ GFP mitoplasts ($n = 5$ each) (Figures 6G and 6H). Importantly, adenovirus-mediated overexpression of WT Bag3 in $Bag3^{+/-}$ myocytes restored peak $I_{MCU}$ to normal ($P = 0.028$ when compared to $Bag3^{+/-}$). These data suggest that adequate levels of Bag3 are necessary to maintain MCU expression and/or activity.

**THE HUMAN PROTEOME AND INFLAMMASOME REFLECT THAT SEEN IN $BAG3^{+/-}$ MICE.** The levels of Bag3 are reduced by approximately 50% in LV

**FIGURE 6 Continued**

Left ventricular myocytes were isolated from $Bag3^{+/-}$ and WT mice and exposed to hypoxia for 30 minutes followed by reoxygenation for 20 minutes as described in the Materials and Methods section. Cells were then permeabilized with digitonin and supplemented with succinate. **(A)** The ratiometric indicator JC-1 was added as indicated by the downward arrow to monitor the mitochondrial membrane potential ($\Delta\Psi_m$). The mitochondrial uncoupler CCCP (2 μM) was added at the second arrow. **(B)** A summary of the $\Delta\Psi_m$ after the addition of $Ca^{2+}$ but before the addition of CCCP ($n = 4$ in each group). **(C)** Extramitochondrial $Ca^{2+}$ was measured in a separate group of myocytes after the addition of the ratiometric dye Fura FF at 0 seconds and the subsequent addition of $Ca^{2+}$ pulses (10 μM) as indicated by the **arrows**. The cytosolic $Ca^{2+}$ clearance rate was then measured after the first $Ca^{2+}$ pulse as fluorescence arbitrary units. **(D)** A summary of the cytosolic $Ca^{2+}$ clearance rate ($n = 4$ for each measure). *$P < 0.05$. ***$P < 0.001$. **(E, F)** The $\Delta\Psi_m$ is generated by $Ca^{2+}$ flux through the $Ca^{2+}$-uniporter that is composed of 5 proteins: MICU1, MICU2, MCUb, MCU, and EMRE. Bag3 haploinsufficiency results in a significant ($P < 0.05$) decrease in the relative levels of MICU1 and a trend towards a decrease in MICU2, which leads to an increase (adverse) in membrane function potential **(E and F)**. **(G, H)** Currents from cardiac mitoplasts ($I_{MCU}$) were recorded before and after application of 5 mM $Ca^{2+}$ to the bath. Currents were measured during a voltage-ramp as indicated. **(G)** Traces are representative single $I_{MCU}$ recordings from WT-GFP, $Bag3^{+/-}$-GFP, and $Bag3^{+/-}$-Bag3 mitoplasts. **(H)** Means ± SEM of $I_{MCU}$ (pA/pF) from WT-GFP ($n = 5$), $Bag3^{+/-}$-GFP ($n = 4$), and $Bag3^{+/-}$- Bag3 ($n = 5$) mitoplasts. *$P < 0.05$. **$P < 0.01$.

myocardium of failing human heart tissue when compared with nonfailing controls (Supplemental Figure 4). Furthermore, we found that the inflammasome of the human heart is similar but not identical to that in mice with haploinsufficiency of Bag3; levels of cPARP (Supplemental Figure 4D) and cleaved caspase-8 (Supplemental Figure 4E) are elevated whereas levels of caspase-3 are not increased (Supplementary Figure 4F). In contrast, we did not see a significant change in HuR with the mice (Supplemental Figure 4G).

## DISCUSSION

Bag3 is present in all living organisms that have been test including plants.[50] Therefore it is not surprising that the full extent of the functional capabilities of Bag3 are not known. Therefore, we took advantage of the availability of young mice in which a single allele of Bag3 was ablated but had not yet developed a decrease in ejection fraction to dissect the many molecular pathways that were modified by Bag3 depletion. As a first step we performed proteomics, to identify previously unrecognized consequences of Bag3 haploinsufficiency.

Bag3 modifies the extrinsic pathways of apoptosis while also serving as a regulator of inflammation through activation of the cardiac inflammasome and, in particular, the TNFR1 signaling cascade. We also report for the first time that Bag3 plays an equally important role in supporting transport of $Ca^{2+}$ into and out of the mitochondria. This transport of $Ca^{2+}$ maintains the mitochondrial membrane potential that is required for $Ca^{2+}$ flux – the biological event that provides the energy required by the enzymes of the tricarboxylic acid (TCA) cycle.

The cellular machinery that enables Bag3 to remove inextricably damaged or diseased organelles and cells from tissues without the collateral damage that occurs when cells die suddenly is complex and involves multiple regulatory pathways. When cell death is programmed as in apoptosis, the cell membrane remains intact throughout the process such that internal enzymes and toxic materials are degraded before the ultimate end of the cell as a functioning organelle. As pointed out by Haudek et al[51] more than a decade ago, 2 canonical pathways regulate apoptosis in the heart: the type I or the type II pathway. The type I (extrinsic or mitochondrial independent) pathway consists of a cascade of events that begins with activation of a death domain receptor such as the TNFR-1 and ends with activation of the executioner caspases-7 and-3. By contrast, in the type II (intrinsic or mitochondrial-dependent) pathway, apoptosis is activated by the release of proapoptotic signals from the mitochondria including cytochrome c and endonuclease g and the subsequent activation of caspase-9 and -3.

Haudek et al[51] proposed that apoptotic cell death does not necessarily occur as a direct result of the activation of the cell death pathways but is due instead to sustained TNF signaling that leads to cell death after 1 or more antiapoptotic proteins become depleted, whereas overexpression of Bcl-2 was sufficient to partially attenuate this pathway. The present study, albeit in a different model system, is highly compatible with the model espoused by Haudek et al[51] as the absence of a full complement of Bag3, a strong antiapoptotic protein, led slowly but inextricably to diminished LV function and eventual cell death. Just as exogenously driven overexpression of TNF activated the apoptotic pathways in the Haudek model,[51] the absence of a full complement of the strongly antiapoptotic Bag3 protein resulted in a very similar phenotype in the Bag3 haploinsufficiency model with an increase in total caspase-3 levels but not an increase in caspase-3 activity. What is unique to the haploinsufficiency of Bag3 model is an increase in the levels of TNF as well as an adverse change (decrease) in the $\Delta\Psi_m$ independent of exogenous TNF. Furthermore, the diminished role of cIAP due to its inability to partner with a full complement of Bag3 is likely a contributing factor in the pathobiology of Bag3 deficiency, but its role in the Haudek model appears less clear.[52] Nonetheless, both models support the concept that an imbalance between apoptosis and survival has severe consequences in the myocardium.

In the canonical pathways of apoptosis, the type 1 pathway is downregulated by inhibitors of apoptosis (IAPs).[53] By contrast, the type 2 pathway is inhibited by the binding of Bag3 to Bcl-2, the founding member of the very large Bcl-2 family of proteins that includes both proapoptotic (BIM, BID, BAD, and BAX/BAK) and anti-apoptotic (Bcl-2, Bcl-$X_L$, and MCL-1) members.[44] In the present study, the loss of 1 allele of Bag3 and the resulting decrease in Bag3 levels by 50% was associated with an increase in caspase-3 but not a change in the ratio of cleaved caspase-3/total caspase-3. Rather, there is a significant increase in the ratio of cleaved caspase-8 to total caspase-8 which is associated with an increase in apoptosis.

Once activated, caspase-8 is responsible for apoptosis induced by the death receptors Fas, TNFR1, and DR3. In fact, in previous studies, deletions of caspase-8 and RIPK3 prevent aberrant cell death, reduce the inflammation, and prolong mouse survival.[52] Caspase-8 has been studied extensively in cancer but less so in the heart.[52,54,55] However, the results of the present study suggest that it may play a greater role in the heart than has been appreciated.

An interesting finding is that cIAP co-immunoprecipitates with Bag3. This association between Bag3 and cIAP is selective as we found that Bag3 does not precipitate with the x-linked homolog XIAP, an inhibitor that directly neutralizes caspase-9 and the effector caspases-3 and -7 and is found in abundance in many different types of advanced cancers.[56] Previous studies in inflammatory bowel disease and in cancer have shown that cIAPs and their antagonists regulate spontaneous and TNF-induced proinflammatory cytokine and chemokine production.[57] Because Bag3 immunoprecipitates with cIAP, and cIAP has previously been shown to couple with the TNFR1 at the critical junction of TRAF2/TRAF5, LUBAC, and RIPK1, we suggest that the role of Bag3 could be a fertile area for future studies aimed at understanding TNF signaling and the inflammasome of myocardial cells.[58]

Surprisingly, Bag3 did not co-immunoprecipitate with SMAC. When SMAC translocates to the cytoplasm, it competes with cIAP, dislodging it, allowing the caspase to be activated. Although our studies suggest that this translocation does not occur in the absence of Bag3, further studies are needed to elucidate the mechanism by which Bag3 regulates SMAC translocation. We also looked to see whether decreased levels of Bag3 led to myofibrillar disarray that has been reported in some patients with Bag3 mutations and DCM.[59] As seen in **Figure 5**, we saw no evidence of myofibrillar disarray in the 8-week-old $BAG3^{+/-}$ mice; however, we did not find this surprising as, in our clinical experience, myofibrillar disarray is often confused with contraction band necrosis, a common finding when hearts are not stopped in diastole. By contrast, myofibrillar disarray is recognized as a characteristic feature of the hearts of patients with the dominant negative P209L Bag3 variant.

The mitochondrial $Ca^{2+}$ ($mCa^{2+}$) uniporter, the major pathway for $Ca^{2+}$ uptake by the mitochondria, plays an important role in the heart as it is responsible for adenotriphosphate production by the TCA cycle and in particular the activity of the $Ca^{2+}$-regulated enzymes of the TCA cycle.[60] In fact, in the present study, we found that the proteomic studies of $Bag3^{+/-}$ mice showed that Bag3 is associated with an increase in the $Ca^{2+}$-dependent tricarboxylic enzymes, including pyruvate dehydrogenase, alpha ketoglutarate dehydrogenase, and isocitrate dehydrogenase.[61]

Supranormal levels of $mCa^{2+}$ result in an increased workload, thereby increasing cell stress.[62] The MCU is the major pathway for $Ca^{2+}$ uptake by the mitochondria, whereas the mitochondrial permeability transition pore is the site through which excess $Ca^{2+}$ is lost. Although it would be attractive to suggest that the decrease in MCU level and activity in $Bag3^{+/-}$ hearts contributes to the HFrEF phenotype, the biology of $mCa^{2+}$ is complex and not without controversy. For example, MCU inhibition was purported to be beneficial in both cardiac hypertrophy and in heart failure with reduced function.[63-65] By contrast, very recent studies in zebra fish, diabetic mouse heart and in a guinea pig model of heart failure showed that restitution of normal or supranormal levels of MCU would have salutary effects on heart function.[66-68] The mechanisms responsible for the molecular and cellular biology of the mitochondria, particularly how it relates $Ca^{2+}$ homeostasis, has also been debated.[53,58,59] In view of the controversy, our observation that restoration of normal levels of Bag3 improves $mCa^{2+}$ uptake and, by extension, enhances cellular bioenergetics, thereby providing benefit to the cell, should be interpreted carefully.

**STUDY LIMITATIONS.** We have not followed the various processes that are activated or inhibited by Bags3 loss for longer periods. Furthermore, we have not provided information regarding the important question of how Bag3 levels are regulated during the stress of failure. However, both we and others have studied the role of Bag3 during the stress of myocardial damage and failure and the increase in knowledge about its roles will hopefully lead to identification of the mechanism or mechanisms that regulate its expression and/or clearance.

## CONCLUSIONS

The importance of our results is that we show for the first time that Bag3 modulates the inflammasome through both canonical and noncanonical pathways, but that it is also is obligatory for the normal function of the mitochondrial membrane and, in particular, the maintenance of the negative charge of the mitochondrial membrane. Thus, it is not difficult to understand

JACC: BASIC TO TRANSLATIONAL SCIENCE VOL. 8, NO. 7, 2023
JULY 2023:820–839

that a loss of 1 allele of Bag3 would have undue consequences for the maintenance of many biological processes and tissues. Thus, a caveat of the present study is that a protein that has no known defined role other than being a chaperone for other proteins causes adverse consequences for multiple organ systems when its levels are diminished. Bag3 is ideally suited for this because of its many protein-protein binding domains, but unlike intracellular proteins that reside in specific domains, Bag3 is found throughout the cell – perhaps in discrete intracellular microenvironments based on its specific responsibilities. The present results expand those niches showing that Bag3 also supports mitochondrial homeostasis through binding to TOM22 and modulates inflammation by stabilizing cIAP. This raises the question of whether Bag3 is multifunctional (performing the same task in multiple situations) or multitasking (executing more than 1 task at the same time). We believe that Bag3 does not fit in either category because it performs the same task (linking 1 protein with another) at the same time yet in different cell types and cellular domains. Perhaps the best description of Bag3 is that it is a universal glue (glus; Latin) that selectively localizes proteins to specific cellular domains where they can interact with colocalized partner proteins. Although not common, the multifunctional protein 4.1R is one example.[69] Further work is needed to better understand how Bag3 itself is regulated in the various cellular compartments and how its role is modified in health and disease.

**ACKNOWLEDGMENTS** All animals used in the experiments detailed in these studies were euthanized by administration of $CO_2$ or nembutol. All studies were approved by the institutional IACUC, and all protocols were up to date at the time of this study. All authors meet the requirements for authorship as proposed by COPE and all approved the final manuscript prior to submission for publication.

## FUNDING SUPPORT AND AUTHOR DISCLOSURES

This work has been supported by a grant from Renovacor, Inc, Greenwich, Connecticut, USA. The work described in this paper was funded in part by a structured research agreement between Renovacor, Inc, and Temple University Office of Technology Transfer. Dr Tomar has received NIH grant K99DK120876. Drs Myers, Cheung, and Feldman have equity in Renovacor, Inc, a public biotechnology company of which Dr Feldman is the Founder and Chief Scientific Advisor. Drs Cheung and Feldman and hold equity in Renovacor. Dr Khalili is the Co-Founder and Chief Scientific Advisor of Excision Bio Therapeutics, Inc, a company that is developing CRISPR-Cas-9-based therapeutics. Drs Cheung, Kirk, and Feldman have submitted a provisional patent to the Temple Office of Technology Transfer and to the Loyola University-Chicago Tech Transfer Office regarding discoveries associated with the present work. Drs Khalili, Cheung, and Feldman held previous U.S. patent #11236389 that was licensed through Temple University to Renovacor, Inc, including U.S. patents #61/934,483 (BAG3 as a target for therapy of heart failure) and #62/205,990 (BAG3 composition and methods), the approval of which is pending. Dr Khalili has licensed technology to Excision. Drs Khalili and Feldman's laboratory work is monitored by a specific member of the Committee on Conflicts of Interest, and each have individual oversight guidelines that govern their relationships with their companies as well as with other investigators in the University. Yearly reports are submitted to the Committee, and the individual member of the committee assigned to their programs meets with Dr Feldman or Dr Khalili annually. For its part, Temple University has significant financial interests in the technology licensed to Renovacor, Inc. The financial interests are being managed in accordance with Temple University's Institutional policy.

**ADDRESS FOR CORRESPONDENCE:** Dr Arthur M. Feldman, Center for Neurovirology and Gene Editing Lewis Katz, School of Medicine, 3500 North Broad Street, MERB 752, Philadelphia, Pennsylvania 19140, USA. E-mail: Arthur.feldman@tuhs.temple.edu.

## PERSPECTIVES

**COMPETENCY IN MEDICAL KNOWLEDGE:** Our growing understanding of the pathobiology of the failing heart has been closely linked with the development of new therapies. For example, the observations that levels of myocardial b-AR, angiotensin-converting enzymes, and natriuretic peptides played a role in determining disease severity was the justification for clinicians to question existing dogma and to develop the first angiotensin receptor blockers, b-AR antagonists, and neprilysin inhibitors, respectively. The evolution of human genomics/genetics and the possibility of gene therapy has raised new questions regarding treatment strategies. Specifically, should gene therapy be tested and eventually used in patients who carry a disease associated variant but have no symptoms, patients with mild disease but no symptoms, or in those with moderate disease and NYHA functional class III symptoms. Using transgenic mice in which one allele of *BAG3* was knocked out, our study shows that before the onset of cardiac dilation and diminished function, there are profound abnormalities in apoptotic signaling and mitochondrial function that predict a poor long-term outcome. This would suggest that the mice might do best with earlier treatment rather than later treatment. Mice will help us to clarify the biology of Bag3; however, important data will also come from the practice community as the use of genomics to predict outcomes and the effectiveness of treatment strategies expands. Understanding the biological nuances that separate patients with 1 variant from those with a different variant in the same gene or a variant in a different gene will be important in selecting the right therapy for each patient.

**TRANSLATIONAL OUTLOOK:** The list of important cellular pathways that are regulated to some degree by the presence or absence of Bag3 continues to expand. In the study reported herein, we find for the first time that Bag3 haploinsufficiency has unrecognized adverse effects on the biology of a cardiac cell that occur before there is a fall in ejection fraction or an increase in LV size. First, the loss of 1 allele of *BAG3* results in enhanced stress-induced apoptosis due in part to an increase in caspase-8. Second, an absence of a full-complement of Bag3 resulted in a decrease in the ability of the cell to maintain the $\Delta\Psi_m$ accompanying changes in uniporter levels (MICU1) and loss of optimal $Ca^{2+}$ transport. And lastly, a deficiency of Bag3 led to diminished binding to TOM22, a critical element for maintaining the continued transport of protein fragments and protein into the mitochondrial inner membrane. That these adverse effects were attributable to a loss of Bag3 was shown by the fact that replacement of Bag3 using an adenoviral vector returned the membrane potential to its previous highly negative (normal) level. These studies set the stage for a new classification of proteins: the intracellular glue. This designation would include any proteins that augment the presence of cognate elements of a reaction in an intracellular domain or microenvironment so that reactions are timely and effective rather than being dependent on random motion. New imaging technology will allow this hypothesis to be tested and additional information will be gained by moving from studies of haploinsufficiency to studies that determine the function of single nucleotide variants — an important step in translating from the laboratory to the patient.

## REFERENCES

**1.** Lee JH, Takahashi T, Yasuhara N, Inazawa J, Kamada S, Tsujimoto Y. Bis, a Bcl-2-binding protein that synergizes with Bcl-2 in preventing cell death. *Oncogene*. 1999;18:6183-6190.

**2.** Takayama S, Xie Z, Reed JC. An evolutionarily conserved family of Hsp70/Hsc70 molecular chaperone regulators. *J Biol Chem*. 1999;274:781-786.

**3.** Behl C. Breaking BAG: the co-chaperone BAG3 in health and disease. *Trends Pharmacol Sci*. 2016;37:672-688.

**4.** De Marco M, Turco MC, Marzullo L. BAG3 in tumor resistance to therapy. *Trends Cancer*. 2020;6:985-988.

**5.** Norton N, Li D, Rieder MJ, et al. Genome-wide studies of copy number variation and exome sequencing identify rare variants in BAG3 as a cause of dilated cardiomyopathy. *Am J Hum Genet*. 2011;88:273-282.

**6.** Shah S, Henry A, Roselli C, et al. Genome-wide association and Mendelian randomisation analysis provide insights into the pathogenesis of heart failure. *Nat Commun*. 2020;11:163.

**7.** Choquet H, Thai KK, Jiang C, et al. Meta-analysis of 26 638 individuals identifies two genetic loci associated with left ventricular ejection fraction. *Circ Genom Precis Med*. 2020;13:e002804.

**8.** Mazzarotto F, Tayal U, Buchan RJ, et al. Reevaluating the genetic contribution of monogenic dilated cardiomyopathy. *Circulation*. 2020;141:387-398.

**9.** Homma S, Iwasaki M, Shelton GD, Engvall E, Reed JC, Takayama S. BAG3 deficiency results in fulminant myopathy and early lethality. *Am J Pathol*. 2006;169:761-773.

**10.** McDermott-Roe C, Lv W, Maximova T, et al. Investigation of a dilated cardiomyopathy- associated variant in BAG3 using genome-edited iPSC-derived cardiomyocytes. *JCI Insight*. 2019;4.

**11.** Fang X, Bogomolovas J, Wu T, et al. Loss-of-function mutations in co-chaperone BAG3 destabilize small HSPs and cause cardiomyopathy. *J Clin Invest*. 2017;127:3189-3200.

**12.** Myers VD, Tomar D, Madesh M, et al. Haploinsufficiency of Bcl2-associated athanogene 3 in mice results in progressive left ventricular dysfunction, beta-adrenergic insensitivity, and

increased apoptosis. *J Cell Physiol*. 2018;233:6319–6326.

**13.** Feldman AM, Begay RL, Knezevic T, et al. Decreased levels of BAG3 in a family with a rare variant and in idiopathic dilated cardiomyopathy. *J Cell Physiol*. 2014;229:1697–1702.

**14.** Toro R, Perez-Serra A, Campuzano O, et al. Familial dilated cardiomyopathy caused by a novel frameshift in the BAG3 gene. *PLoS One*. 2016;11:e0158730.

**15.** Rosati A, Graziano V, De Laurenzi V, Pascale M, Turco MC. BAG3: a multifaceted protein that regulates major cell pathways. *Cell Death Dis*. 2011;2:e141.

**16.** De Marco M, Basile A, Iorio V, et al. Role of BAG3 in cancer progression: a therapeutic opportunity. *Semin Cell Dev Biol*. 2018;78:85–92.

**17.** Sherman MY, Gabai V. The role of Bag3 in cell signaling. *J Cell Biochem*. 2022;123(1):43–53.

**18.** Hockenbery D, Nunez G, Milliman C, Schreiber RD, Korsmeyer SJ. Bcl-2 is an inner mitochondrial membrane protein that blocks programmed cell death. *Nature*. 1990;348:334–336.

**19.** Feldman AM, Gordon J, Wang J, et al. BAG3 regulates contractility and Ca(2+) homeostasis in adult mouse ventricular myocytes. *J Mol Cell Cardiol*. 2016;92:10–20.

**20.** Martin TG, Tawfik S, Moravec CS, Pak TR, Kirk JA. BAG3 expression and sarcomere localization in the human heart are linked to HSF-1 and are differentially affected by sex and disease. *Am J Physiol Heart Circ Physiol*. 2021;320(6):H2339–H2350.

**21.** Kimura K, Ooms A, Graf-Riesen K, et al. Overexpression of human BAG3(P209L) in mice causes restrictive cardiomyopathy. *Nat Commun*. 2021;12:3575.

**22.** Shy M, Rebelo AP, Feely SM, et al. Mutations in BAG3 cause adult-onset Charcot-Marie-tooth disease. *J Neurol Neurosurg Psychiatry*. 2018;89:313–315.

**23.** Quintana MT, Parry TL, He J, et al. Cardiomyocyte-specific human Bcl2-associated anthanogene 3 P209L expression induces mitochondrial fragmentation, Bcl2-associated anthanogene 3 haploinsufficiency, and activates p38 signaling. *Am J Pathol*. 2016;186:1989–2007.

**24.** Fang X, Bogomolovas J, Zhou PS, et al. P209L mutation in Bag3 does not cause cardiomyopathy in mice. *Am J Physiol Heart Circ Physiol*. 2019;316:H392–H399.

**25.** Bristow MR, Minobe WA, Raynolds MV, et al. Reduced beta 1 receptor messenger RNA abundance in the failing human heart. *J Clin Invest*. 1993;92:2737–2745.

**26.** Li YY, Feldman AM, Sun Y, McTiernan CF. Differential expression of tissue inhibitors of metalloproteinases in the failing human heart. *Circulation*. 1998;98:1728–1734.

**27.** Huang DW, Sherman BT, Tan Q, et al. DAVID bioinformatics resources: expanded annotation database and novel algorithms to better extract biology from large gene lists. *Nucleic Acids Res*. 2007;35:W169–W175.

**28.** Huang da W, Sherman BT, Lempicki RA. Systematic and integrative analysis of large gene lists using DAVID bioinformatics resources. *Nat Protoc*. 2009;4:44–57.

**29.** Su F, Myers VD, Knezevic T, et al. Bcl-2-associated athanogene 3 protects the heart from ischemia/reperfusion injury. *JCI Insight*. 2016;1:e90931.

**30.** Brinks H, Boucher M, Gao E, et al. Level of G protein-coupled receptor kinase-2 determines myocardial ischemia/reperfusion injury via pro- and anti-apoptotic mechanisms. *Circ Res*. 2010;107:1140–1149.

**31.** Zhou YY, Wang SQ, Zhu WZ, et al. Culture and adenoviral infection of adult mouse cardiac myocytes: methods for cellular genetic physiology. *Am J Physiol Heart Circ Physiol*. 2000;279:H429–H436.

**32.** Song J, Zhang XQ, Wang J, et al. Regulation of cardiac myocyte contractility by phospholemman: Na+/Ca2+ exchange versus Na+ -K+ -ATPase. *Am J Physiol Heart Circ Physiol*. 2008;295:H1615–H1625.

**33.** Wang J, Gao E, Rabinowitz J, et al. Regulation of in vivo cardiac contractility by phospholemman: role of Na+/Ca2+ exchange. *Am J Physiol Heart Circ Physiol*. 2011;300:H859–H868.

**34.** Zhu W, Tilley DG, Myers VD, Coleman RC, Feldman AM. Arginine vasopressin enhances cell survival via a G protein-coupled receptor kinase 2/beta-arrestin1/extracellular-regulated kinase 1/2-dependent pathway in H9c2 cells. *Mol Pharmacol*. 2013;84:227–235.

**35.** Tilley DG, Zhu W, Myers VD, et al. Beta-adrenergic receptor-mediated cardiac contractility is inhibited via vasopressin type 1A-receptor-dependent signaling. *Circulation*. 2014;130:1800–1811.

**36.** Cheung JY, Thompson IG, Bonventre JV. Effects of extracellular calcium removal and anoxia on isolated rat myocytes. *Am J Physiol*. 1982;243:C184–C190.

**37.** Tucker AL, Song J, Zhang XQ, et al. Altered contractility and [Ca2+]i homeostasis in phospholemman-deficient murine myocytes: role of Na+/Ca2+ exchange. *Am J Physiol Heart Circ Physiol*. 2006;291:H2199–H2209.

**38.** Miller BA, Hoffman NE, Merali S, et al. TRPM2 channels protect against cardiac ischemia-reperfusion injury: role of mitochondria. *J Biol Chem*. 2014;289:7615–7629.

**39.** Kirichok Y, Krapivinsky G, Clapham DE. The mitochondrial calcium uniporter is a highly selective ion channel. *Nature*. 2004;427:360–364.

**40.** Hoffman NE, Chandramoorthy HC, Shamugapriya S, et al. MICU1 motifs define mitochondrial calcium uniporter binding and activity. *Cell Rep*. 2013;5:1576–1588.

**41.** Fang X, Bogomolovas J, Trexler C, Chen J. The BAG3-dependent and -independent roles of cardiac small heat shock proteins. *JCI Insight*. 2019;4(4):e126464.

**42.** Tahrir FG, Knezevic T, Gupta MK, et al. Evidence for the role of BAG3 in mitochondrial quality control in cardiomyocytes. *J Cell Physiol*. 2017;232:797–805.

**43.** Liu G, Zou H, Luo T, et al. Caspase-dependent and caspase-independent pathways are involved in cadmium-induced apoptosis in primary rat proximal tubular cell culture. *PLoS One*. 2016;11:e0166823.

**44.** Mastrocola R, Aragno M, Alouatta G, Collino M, Penna C, Pagliaro P. Metaflammation: tissue- specific alterations of the NLRP3 inflammasome platform in metabolic syndrome. *Curr Med Chem*. 2018;25:1294–1310.

**45.** Mashimo M, Bu X, Aoyama K, et al. PARP1 inhibition alleviates injury in ARH3-deficient mice and human cells. *JCI Insight*. 2019;4(4):e124519.

**46.** Romero-Becerra R, Santamans AM, Folgueira C, Sabio G. p38 MAPK pathway in the heart: new insights in health and disease. *Int J Mol Sci*. 2020;21(19):7412.

**47.** Green LC, Anthony SR, Slone S, et al. Human antigen R as a therapeutic target in pathological cardiac hypertrophy. *JCI Insight*. 2019;4(4):e121541.

**48.** Krishnamurthy P, Lambers E, Verma S, et al. Myocardial knockdown of mRNA-stabilizing protein HuR attenuates post-MI inflammatory response and left ventricular dysfunction in IL-10-null mice. *FASEB J*. 2010;24:2484–2494.

**49.** Mammucari C, Gherardi G, Rizzuto R. Structure, activity regulation, and role of the mitochondrial calcium uniporter in health and disease. *Front Oncol*. 2017;7:139.

**50.** Doukhanina EV, Chen S, van der Zalm E, Godzik A, Reed J, Dickman MB. Identification and functional characterization of the BAG protein family in *Arabidopsis thaliana*. *J Biol Chem*. 2006;281:18793–18801.

**51.** Haudek SB, Taffet GE, Schneider MD, Mann DL. TNF provokes cardiomyocyte apoptosis and cardiac remodeling through activation of multiple cell death pathways. *J Clin Invest*. 2007;117:2692–2701.

**52.** Zhang J, Webster JD, Dugger DL, et al. Ubiquitin ligases cIAP1 and cIAP2 limit cell death to prevent inflammation. *Cell Rep*. 2019;27:2679–2689e3.

**53.** Siddiqui WA, Ahad A, Ahsan H. The mystery of BCL2 family: Bcl-2 proteins and apoptosis: an update. *Arch Toxicol*. 2015;89:289–317.

**54.** Baumgartner HK, Gerasimenko JV, Thorne C, et al. Caspase-8-mediated apoptosis induced by oxidative stress is independent of the intrinsic pathway and dependent on cathepsins. *Am J Physiol Gastrointest Liver Physiol*. 2007;293:G296–G307.

**55.** Kruidering M, Evan GI. Caspase-8 in apoptosis: the beginning of "the end". *IUBMB Life*. 2000;50:85–90.

**56.** Obexer P, Ausserlechner MJ. X-linked inhibitor of apoptosis protein — a critical death resistance regulator and therapeutic target for personalized cancer therapy. *Front Oncol*. 2014;4:197.

**57.** Kearney CJ, Sheridan C, Cullen SP, et al. Inhibitor of apoptosis proteins (IAPs) and their antagonists regulate spontaneous and tumor necrosis factor (TNF)–induced proinflammatory

cytokine and chemokine production. *J Biol Chem*. 2013;288:4878–4890.

**58.** Brenner D, Blaser H, Mak TW. Regulation of tumour necrosis factor signalling: live or let die. *Nat Rev Immunol*. 2015;15:362–374.

**59.** Dominguez F, Cuenca S, Bilinska Z, et al. Dilated cardiomyopathy due to BLC2-associated athanogene 3 (BAG3) mutations. *J Am Coll Cardiol*. 2018;72:2471–2481.

**60.** Liu T, O'Rourke B. Regulation of mitochondrial Ca2+ and its effects on energetics and redox balance in normal and failing heart. *J Bioenerg Biomembr*. 2009;41:127–132.

**61.** Maack C, Cortassa S, Aon MA, Ganesan AN, Liu T, O'Rourke B. Elevated cytosolic Na+ decreases mitochondrial Ca2+ uptake during excitation-contraction coupling and impairs energetic adaptation in cardiac myocytes. *Circ Res*. 2006;99:172–182.

**62.** Liu T, Yang N, Sidor A, O'Rourke B. MCU Overexpression rescues inotropy and reverses heart failure by reducing SR Ca(2+) leak. *Circ Res*. 2021;128:1191–1204.

**63.** Tang Y, Wu Y. Decreased ATP production during mitochondrial calcium uniporter inhibition enhances autophagy and mitophagy to provide cardioprotection in cardiac failure. *Int J Cardiol*. 2019;282:67.

**64.** Yu Z, Chen R, Li M, et al. Mitochondrial calcium uniporter inhibition provides cardioprotection in pressure overload-induced heart failure through autophagy enhancement. *Int J Cardiol*. 2018;271:161–168.

**65.** Langenbacher AD, Shimizu H, Hsu W, et al. Mitochondrial calcium uniporter deficiency in zebrafish causes cardiomyopathy with arrhythmia. *Front Physiol*. 2020;11:617492.

**66.** Suarez J, Cividini F, Scott BT, et al. Restoring mitochondrial calcium uniporter expression in diabetic mouse heart improves mitochondrial calcium handling and cardiac function. *J Biol Chem*. 2018;293:8182–8195.

**67.** Garbincius JF, Elrod JW. Is the failing heart starved of mitochondrial calcium? *Circ Res*. 2021;128:1205–1207.

**68.** Pan X, Liu J, Nguyen T, et al. The physiological role of mitochondrial calcium revealed by mice lacking the mitochondrial calcium uniporter. *Nat Cell Biol*. 2013;15:1464–1472.

**69.** Huang SC, Vu LV, Yu FH, Nguyen DT, Benz EJ Jr. Multifunctional protein 4.1R regulates the asymmetric segregation of Numb during terminal erythroid maturation. *J Biol Chem*. 2021;297:101051.

**KEY WORDS** apoptosis, Bcl2-associated athanogene-3, caspase, metabolism, tumor necrosis factor

**APPENDIX** For an expanded Materials and Methods section as well as a supplemental table and figures, please see the online version of this paper.